Age-Related Changes of Regional Pulse Wave Velocity in the Descending Aorta Using Fourier Velocity Encoded M-Mode

Valentina Taviani,[1]* Stacey S. Hickson,[2] Christopher J. Hardy,[3] Carmel M. McEniery,[2] Andrew J. Patterson,[1] Jonathan H. Gillard,[1] Ian B. Wilkinson,[2] and Martin J. Graves[1]

Aortic pulse wave velocity (PWV) is an independent determinant of cardiovascular risk. Although aortic stiffening with age is well documented, the interaction between aging and regional aortic PWV is still a debated question. We measured global and regional PWV in the descending aorta of 56 healthy subjects aged 25–76 years using a one-dimensional, interleaved, Fourier velocity encoded pulse sequence with cylindrical excitation. Repeatability across two magnetic resonance examinations (n = 19) and accuracy against intravascular pressure measurements (n = 4) were assessed. The global PWV was found to increase nonlinearly with age. The thoracic aorta was found to stiffen the most with age (PWV [thoracic, 20–40 years] = 4.7 ± 1.1 m/s; PWV [thoracic, 60–80 years] = 7.9 ± 1.5 m/s), followed by the mid- (PWV [mid-abdominal, 20–40 years] = 4.9 ± 1.3 m/s; PWV [mid-abdominal, 60–80 years] = 7.4 ± 1.9 m/s) and distal abdominal aorta (PWV [distal abdominal, 20–40 years] = 4.8 ± 1.4 m/s; PWV [distal abdominal, 60–80 years] = 5.7 ± 1.4 m/s). Good agreement was found between repeated magnetic resonance measurements and between magnetic resonance PWVs and the gold-standard. Fourier velocity encoded M-mode allowed to measure global and regional PWV in the descending aorta. There was a preferential stiffening of the thoracic aorta with age, which may be due to progressive fragmentation of elastin fibers in this region. Magn Reson Med 65:261–268, 2011. © 2010 Wiley-Liss, Inc.

Key words: regional pulse wave velocity; aortic stiffness; aging; Fourier velocity encoding

INTRODUCTION

Central arteries like the aorta play a crucial role in buffering and attenuating the pulsatile nature of blood flow (1). Over time, the aorta gets stiffer (2), dilates and becomes more tortuous (3). Stiffening of the aorta is associated with increased pulse pressure, which promotes ventricular stiffening and hypertrophy, ultimately leading to diastolic dysfunction and heart failure (4).

Increased aortic stiffness has also been found to be associated with a variety of physiological conditions (low birth weight (5), menopausal status (6), lack of physical activity (7)), genetic background (8), traditional cardiovascular risk factors such as obesity (9), smoking (10), hypertension (11), hypercholesterolemia (12) and diabetes (13), and non-cardiovascular diseases like end-stage renal disease (14), chronic kidney disease (15), rheumatoid arthritis (16), systemic vasculitis (17) and Marfan syndrome (18). Arterial stiffening has also been recently recognized as an independent determinant of cardiovascular risk, with aortic pulse wave velocity (PWV) capable of predicting future cardiovascular events in a variety of populations independently of blood pressure (19).

The structure and composition of the aortic wall varies significantly along the length of the aorta (20). Although aortic stiffening with age has been extensively documented (2,21), the interplay between ageing and regional compliance is still a debated question, with major implications for therapeutic interventions.

Previous magnetic resonance (MR) studies have addressed the problem of quantifying regional arterial compliance either by direct measurement of arterial distensibility (22–24) or by PWV measurement using cine phase contrast (CPC) with through-plane velocity encoding (18,25,26). Direct measurements of arterial distensibility are limited by the difficulty in evaluating local pulse pressure. The accuracy of PWV measurements by CPC with through-plane velocity encoding can be degraded when short arterial segments are considered, due to the limited temporal resolution of CPC. In addition, the long acquisition time per imaged slice means that regional PWV is often estimated on the basis of the transit time between the two extremities of a given arterial segment, with no information acquired at intermediate points. Rogers et al. used CPC with in-plane velocity encoding performed in an oblique-sagittal long-axis view of the aorta (27). However, only the velocity information corresponding to four predefined anatomical locations was used to measure regional PWV.

Fourier velocity encoded (FVE) M-mode is an interleaved one-dimensional MR technique which can produce time-velocity profiles with high temporal and spatial resolution along a relatively straight arterial segment (28). Time-velocity profiles are acquired for each point along a relatively long segment, which is then divided into smaller segments to obtain localized

[1]Department of Radiology, University of Cambridge, Addenbrooke's Hospital, Cambridge, United Kingdom.

[2]Clinical Pharmacology Unit, University of Cambridge, Addenbrooke's Hospital, Cambridge, United Kingdom.

[3]GE Global Research, Niskayuna, New York.

Grant sponsors: Department of Health through the National Institute for Health Research Comprehensive Biomedical Research Centre (award to Cambridge University Hospitals NHS Foundation Trust in partnership with the University of Cambridge), EPSRC DTA and Cambridge European Trust.

*Correspondence to: Valentina Taviani, MSc., University Department of Radiology, Addenbrooke's Hospital, Hills Road, Box 218, Cambridge CB2 0QQ, UK. E-mail: vt232@cam.ac.uk

Received 17 March 2010; revised 17 June 2010; accepted 7 July 2010.

DOI 10.1002/mrm.22590

Published online 27 September 2010 in Wiley Online Library (wileyonlinelibrary.com).

Table 1
Characteristics of Subjects

Variable	Value (mean ± std)
Age (yrs)	53 ± 16
Height (cm)	170 ± 9
Weight (kg)	74 ± 8
Heart rate (bpm)	66 ± 11
Brachial supine diastolic BP (mm Hg)	73 ± 7
Brachial supine systolic BP (mm Hg)	125 ± 14
Brachial MAP (mm Hg)	90 ± 9

BP, blood pressure; MAP, mean arterial pressure.

measurements of PWV. In the descending aorta, FVE M-mode-derived PWVs have been shown to be more repeatable than CPC-derived PWVs, due to the higher temporal and spatial resolution achievable with FVE M-mode (29). In case of localized measurements, PWVs obtained from the slope of the best fit line to data representing position of the foot of the wave as a function of position along the vessel are expected to be more robust than measurements based on two-point transit-time estimates.

In this work, we measured regional PWV in the descending aorta using FVE M-mode in a large cohort of healthy subjects. Our aim was to investigate the interaction between regional aortic stiffening and age.

MATERIALS AND METHODS

Patient Population

Fifty-six healthy subjects (29 men; age range: 25–76 years, mean age: 53 years) participated in the study (Table 1). All subjects were normotensive and free from known cardiovascular disease and medication. Accuracy of the MR-derived PWV values was tested in a separate cohort of four patients undergoing intravascular pressure measurements (3 men; age range: 58–78 years, mean age: 69 years). Approval was obtained from the local Research Ethics Committee and all participants gave written informed consent.

Image Acquisition

Images were acquired on an 8-channel 1.5T whole-body imaging system (Signa HDx, GE Healthcare, Waukesha, WI) using a 12-element abdo-torso phased-array surface coil, with the elements (18 cm long in the SI direction and 25 cm wide in the LR direction) arranged into two 3 × 2 arrays. An ECG-triggered, oblique-sagittal, double inversion recovery prepared fast spin-echo (FSE) sequence was used to localize the descending aorta (Fig. 1a).

The FVE M-mode sequence consisted of a cylindrical excitation pulse (30), followed by a bipolar velocity-encoding gradient and a readout gradient applied along the axis of the cylinder or pencil (28) (Fig. 2). The sequence was gated to the cardiac R-wave and executed 32 times per heart cycle with the bipolar flow encoding gradient amplitude stepped to a new value on each new trigger. To increase the effective temporal resolution to 3.5 ms, four interleaves of the data were acquired, resulting in 128 time frames covering the first 450 ms of the cardiac cycle. Thirty-two velocity-encoding steps were used, yielding a true velocity resolution of 9.4 cm/s,

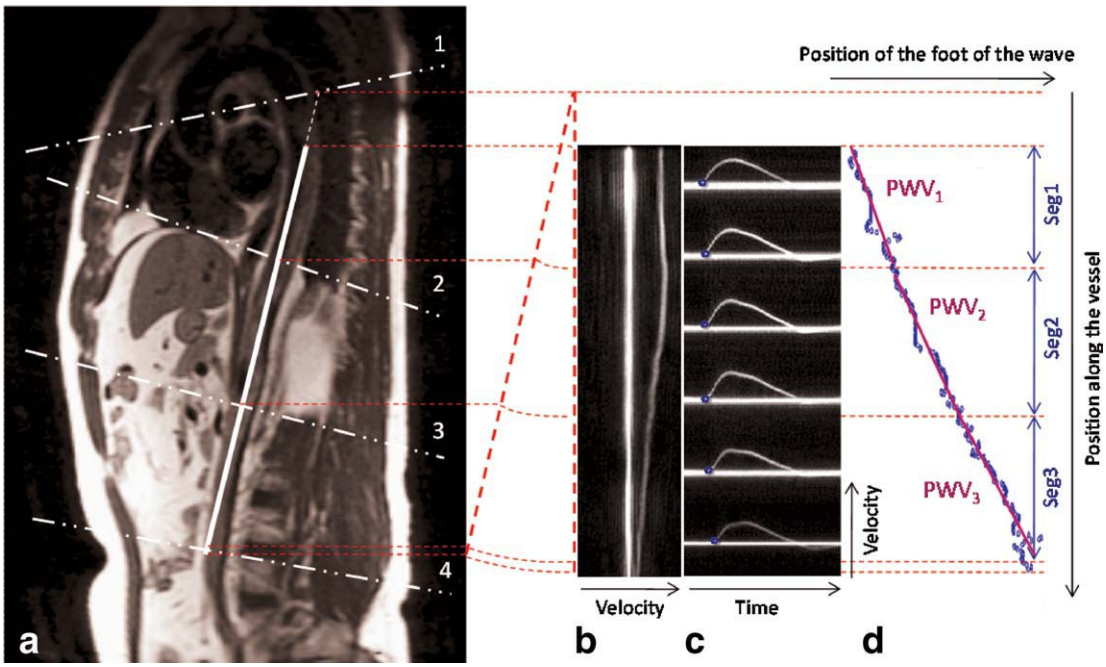

FIG. 1. **a**: Localization of the aorta and prescription of the Fourier velocity encoded (FVE) M-mode pulse sequence (solid line); **b**: FVE M-mode image for an early cardiac phase showing the velocity distribution as a function of position along the pencil; **c**: FVE M-mode images reformatted to yield Doppler-like time-velocity traces; **d**: global and regional pulse wave velocities computed by best fit of the data representing position of the foot of the wave versus position along the vessel for the entire length of the pencil and for the three segments defined by the four planes in (a), respectively.

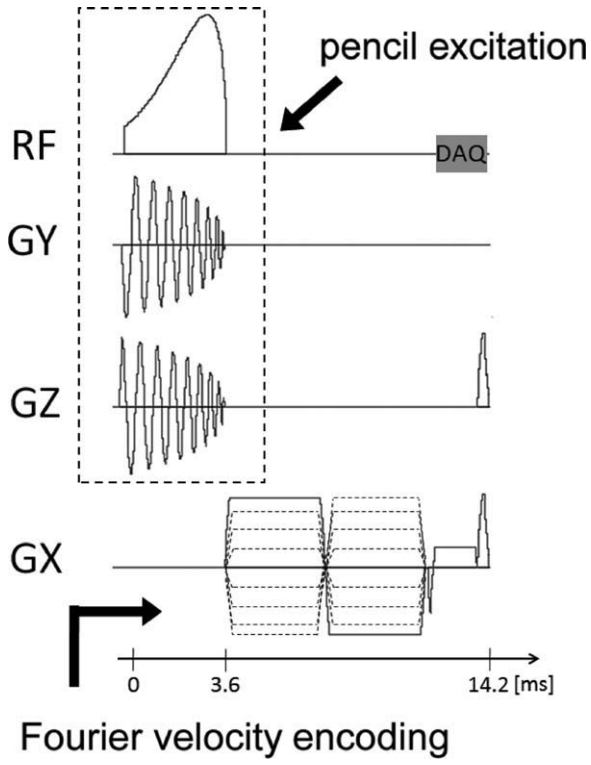

FIG. 2. ECG-gated Fourier velocity encoded (FVE) M-mode pulse sequence comprises 2D pencil excitation pulse followed by stepped bipolar velocity encoding gradient and readout gradient oriented along the pencil axis. Two-dimensional Fourier transformation of the data results in a plot of velocity distribution versus position along the pencil.

which resulted in aliasing of velocities greater than 150 cm/s. The data were zero-filled to 64 lines in the velocity direction, so that 32 velocity encoding steps covered 64 pixels in the reconstructed image. A 24 cm readout field of view (matrix size = 256 × 32), 20° flip angle and a 2 cm diameter cylindrical excitation pulse achieved through an 8-cycle spiral trajectory were prescribed. The inner aliasing ring diameter was 28.5 cm. The average acquisition time was 32 heart beats ×4 interleaves = 128 heart beats (~2 minutes).

Image Analysis

Images were analyzed using a graphical user interface developed in-house using Matlab version 7.5.0 (The Mathworks, Natick, MA). Figure 1b shows an FVE M-mode image corresponding to an early cardiac phase, with the vertical straight line representing static tissue and horizontal displacements being proportional to velocity at that cardiac phase. FVE M-mode images were reformatted to yield Doppler-like time-velocity traces (Fig. 1c) along the length of the pencil (31).

Since velocity measurements were limited to the first half of the R-R interval, plug flow was observed in most of the acquired cardiac phases. In the presence of plug flow, the mean cross-sectional velocity was almost identical to the modal velocity, represented by the locus of maximum-intensity pixels located above the static-tissue signal component. An automatic line detector was used to extract the modal velocity pattern as a function of time from each of the time-velocity images. The resulting velocity profiles, corresponding to different spatial locations along the aorta, were visualized as a velocity surface, each point of which represented velocity at a given time and position. When necessary, a gradient-based regularization technique (32) was used to smooth the obtained velocity surface, with the amount of smoothing kept to a minimum and verified by visual comparison with the original data points (29). The foot of the velocity wave was defined at each spatial location as the intersection between a line fitted to the early systolic upslope (10–40% of peak velocity) and the zero velocity line.

Four planes, orthogonal to the descending aorta, were defined on the FSE scout image: (1) 2 cm distal to the aortic valve (distance measured along the centreline of the ascending aorta); (2) at the level of the diaphragm; (3) midway between location 2 and a location 3 cm proximal to the aortic bifurcation; (4) 3 cm above the aortic bifurcation (Fig. 1a). PWV was computed over the entire length of the pencil and for the three segments delimited by these planes (Seg1 delimited by planes 1 and 2; Seg2 delimited by planes 2 and 3; Seg3 delimited by planes 3 and 4), by linear regression of the position of the foot of the wave as a function of the corresponding location along the aorta (Fig. 1d).

Accuracy

Accuracy of the MR-derived PWVs (global and regional) was tested against the PWV values derived from intravascular pressure measurements. The MR examination was performed within 2 weeks from catheterization. Intravascular measurements were obtained under fluoroscopic guidance using 5F solid-state catheters incorporating a high-fidelity pressure sensor in their tip (Millar Instruments, TX). ECG and pressure waveforms were simultaneously recorded every 10 cm during the catheter pullback, from 1 cm distal to the aortic valve down to the femoral artery, through which the catheter was inserted.

Pressure waveforms were recorded at a sampling rate of 2 kHz. Only pressures recorded within the descending aorta were analyzed. At each recording site, 10–15 cardiac cycles were averaged. The foot of the wave was defined at the intersection between a line fitted to the early systolic upslope (10–40% of peak pressure) and a horizontal line through the minimum pressure occurring in the time interval between the ECG R-wave and the peak systolic pressure. Regional PWVs were computed as $\Delta s/\Delta t$ where Δs and Δt are the distance (10 cm) and transit time between two consecutive recording sites. The global PWV was computed from the slope of the line fitted to the graph showing position of the foot of the wave versus position along the vessel at the recording sites within the descending aorta.

Repeatability

Repeatability was tested on a subset of 19 healthy subjects (included in the study) across two MR

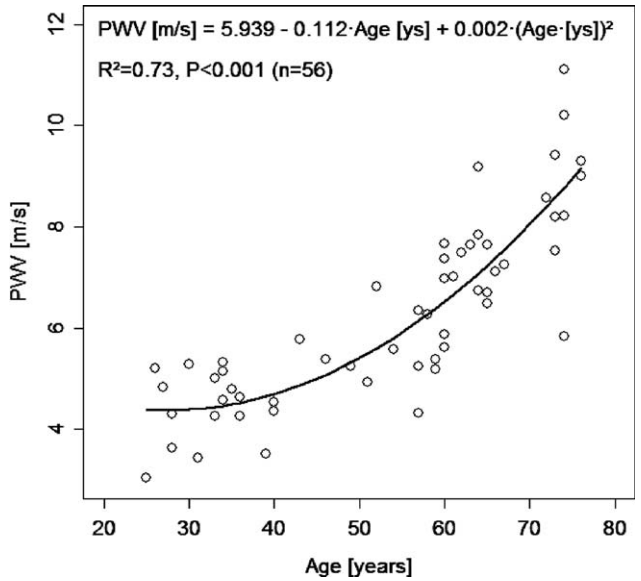

FIG. 3. Global pulse wave velocity showing a markedly nonlinear increase with age. The regression equation obtained using a second-order polynomial model, together with the adjusted R^2 and P-value relative to the F statistics used to test significance, are also reported.

examinations (10 men; age range: 25–57 years, mean age: 38 years). After completion of the MR protocol, each subject was removed and repositioned into the magnet bore and the same MR protocol was repeated.

Statistical Analysis

Results were reported as mean ± standard deviation. Subjects were divided into three age groups: 20–40 years (18 subjects), 40–60 years (17 subjects), and 60–80 years (21 subjects). The significance of differences in PWV between different aortic regions was assessed using a one-way analysis of variance (ANOVA). One-way ANOVA was also used to assess significance of differences in global PWV between the three age groups. A two-way ANOVA was used to test the effects of age and site of increased stiffening on PWV. Age was modeled as a continuous variable. Where significant overall differences existed, a paired two-sided t-test was used to compare between aortic regions within age groups. A P-value less than 0.05 was considered to be significant. The relation between age and position along the aorta was investigated deriving regression equations with first- and second-order polynomial models and the F-test.

The mean of the differences between MR-derived PWVs and the values obtained from intravascular pressure measurements (bias), together with the 95% limits of agreement (LOA) defined as the bias $\pm 1.96 \times$ the standard deviation of the differences, were used to quantify accuracy of the global and regional PWVs. Repeatability was reported according to the definition of Bland and Altman as $2.77 \times$ the within-subject standard deviation σ_w (33).

All the analysis was performed using the statistical programming language R version 2.5.1 (The R Foundation for Statistical Computing, Vienna, Austria).

RESULTS

The global PWV was found to increase nonlinearly with age (Fig. 3). The regression equations using first-and second-order polynomial models were: PWV [m/s] = 1.227 + 0.094 Age [yrs] ($R^2 = 0.68$, $P < 0.001$) and PWV [m/s] = 5.939 − 0.112 Age [yrs] + 0.002 (Age [yrs])^2 ($R^2 = 0.73$, $P < 0.001$), respectively. There was a significant difference in the global PWV between the three age groups (20–40 years: PWV = 4.2 ± 0.7 m/s; 40–60 years: PWV = 5.9 ± 0.9 m/s; 60–80 years: PWV = 8.0 ± 1.3 m/s; $P < 0.001$). There were no differences between genders.

There was a significant difference ($P = 0.004$, one-way ANOVA) between regional PWV in the thoracic aorta (Seg1, PWV = 6.4 ± 2.1 m/s), in the mid-abdominal aorta (Seg2, PWV = 6.0 ± 1.9 m/s) and in the distal abdominal aorta (Seg3, PWV = 5.2 ± 1.5 m/s). Regional PWVs in the thoracic and mid-abdominal aorta were not significantly different ($P = 0.1$).

A significant interaction was found between age and site of increased stiffening ($P = 0.006$, two-way ANOVA, Fig. 4). The thoracic aorta was found to stiffen the most with age (PWV [Seg1, 20–40 years] = 4.7 ± 1.1 m/s; PWV [Seg1, 40–60 years] = 6.2 ± 2.2 m/s; PWV [Seg1, 60–80 years] = 7.9 ± 1.5 m/s), followed by the mid-(PWV [Seg2, 20–40 years] = 4.9 ± 1.3 m/s; PWV [Seg2, 40–60 years] = 5.5 ± 1.3 m/s; PWV [Seg2, 60–80 years] = 7.4 ± 1.9 m/s) and distal abdominal aorta (PWV [Seg3, 20–40 years] = 4.8 ± 1.4 m/s; PWV [Seg3, 40–60 years] = 4.9 ± 1.8 m/s; PWV [Seg3, 60–80 years] = 5.7 ± 1.4 m/s). Within the first and second age group (20–40 years and 40–60 years, respectively) regional PWVs were not significantly different. Within the 60–80 years age group, PWV in the distal abdominal aorta was different from

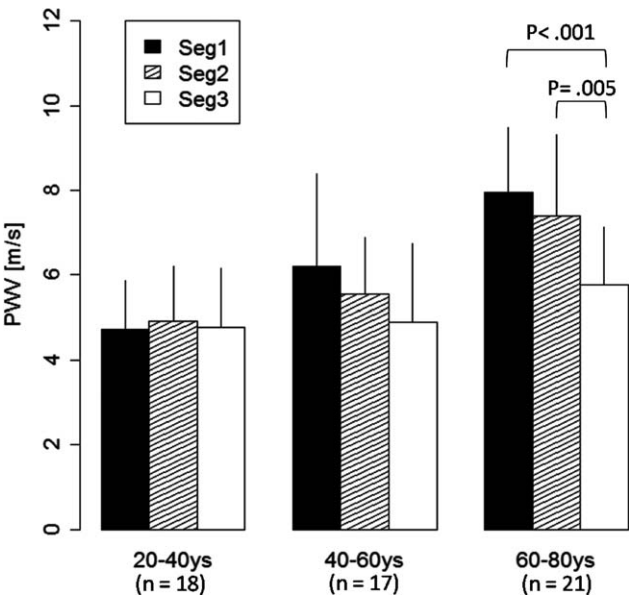

FIG. 4. Regional pulse wave velocity in the thoracic (Seg1), mid (Seg2) and distal abdominal (Seg3) aorta for the different age groups, showing a significant interplay between age and site of age-related increased stiffening ($P = 0.006$, two-way ANOVA).

Table 2
Regional and Global PWV Values as Obtained from MR and Intravascular Pressure Measurements Performed in the Four Patients Undergoing Cardiac Catheterization (PWV values listed as MR/cath)

	PWV					
	Seg1 (m/s)	Seg2 (m/s)	Seg3 (m/s)	Global (m/s)	Age (yrs)	MAP (mm Hg)
Subject 1	4.82/6.29	6.03/6.0	na[a]/10.11	6.78/6.94	71	52
Subject 2	5.29/5.50	7.65/5.28	na[a]/11.36	6.57/5.38	67	78
Subject 3	8.26/8.31	7.75/8.23	8.97/15.37[b]	7.86/8.27	77	78
Subject 4	na[a]/7.46	na[a]/5.92	5.22/4.55	5.22/5.15	58	28

[a]MR measurement not available due to poor image quality or lack of signal caused by pencil mispositioning.
[b]Value referring to a segment stretching 3 cm into the iliac arteries.

the PWV in the thoracic ($P < 0.001$) and in the mid-abdominal aorta ($P = 0.005$).

Accuracy

There was good agreement between MR-derived PWVs and the PWV values obtained from intravascular pressure measurements ($n = 4$, Table 2). The bias was −0.17 m/s and −0.03 m/s for global and regional PWV, respectively. The 95% LOA were −1.55 to 1.21 m/s (range = 2.76 m/s) and −2.52 to 2.45 m/s (range = 4.97 m/s) for global and regional PWV, respectively. Regional PWV accuracy over the three different segments separately was not quantified due to the small sample size.

Repeatability

Repeated measurements of global and regional PWVs were in good agreement ($n = 19$). The within-subject standard deviation was 0.50 m/s and 0.53 m/s for global and regional PWV, respectively. Repeatability of the global and regional PWV measurements was 1.40 m/s and 1.48 m/s, respectively. Repeatability over the entire length of the pencil and the thoracic, mid-abdominal and distal abdominal regions is summarized in Table 3. Repeatability was similar in all segments, although marginally lower in the mid-abdominal aorta (within-subject standard deviation = 0.62 m/s; repeatability = 1.71 m/s).

DISCUSSION

Global and regional PWVs were measured in the descending aorta of 56 healthy subjects using an interleaved one-dimensional MR pulse sequence, which allowed visualization of the flow velocity profile with high temporal and spatial resolution along the vessel. A marked nonlinear increase of the global PWV with age was observed, as previously reported by McEniery et al. (2) and Mitchell et al. (21). Regional PWV was found to decrease towards the periphery, although the difference between the thoracic and mid-abdominal aorta was not significant. The thoracic aorta stiffened the most with age, followed by the mid- and distal-abdominal aorta.

Previous studies of regional aortic PWV often found contrasting results, probably due to the different methodologies used and the small sample size. McDonald derived regional aortic PWVs in four dogs from intravascular pressure measurements and reported increased PWVs away from the heart (34). Similar results were reported by Guo and Kassab, who measured arterial compliance along the aorta of seven mice and found the distal abdominal region to be significantly stiffer than the proximal descending thoracic region (35). These and other early invasive studies performed in canine models (36,37) suggested an increased stiffness towards the periphery, reflecting increased collagen and decreased elastin away from the heart. Although invasive studies are often regarded as the gold standard for PWV measurement, extension of results obtained in animal studies to the human species is hampered by the existence of physiological differences between species and other factors related to the small sample size and narrow age range which are often characteristic of these works.

Human studies performed to date are quite limited and characterized by marginal significance. Latham et al. (38) and Ting et al. (39) used micromanometers mounted on catheters to measure pressure waveforms and hence regional aortic PWV in nine and eight normotensive subjects, respectively. Neither of these studies found statistically significant differences between the thoracic, mid-abdominal and distal-abdominal regions (38,39), although they both found a moderate increase in PWV moving down the aorta, from the arch region to the level of the femoral arteries. All the patients included in these studies were in their forties. This work and previous MR studies (24,27) found no difference between aortic regional PWV in the young, with regional variations becoming evident only in the elderly. Although patients were grouped according to different criteria in these studies, with the "young" group extending up to 55, 30, and 40 years in Rogers et al. (27), Nelson et al. (24) and this study, respectively, the main result that no differences in regional PWV were found in younger individuals was substantially in agreement with the invasive measurements performed by Latham and Ting.

Previous MR studies of regional aortic stiffness used either cine gradient echo techniques (11,22,24) or CPC

Table 3
Repeatability of Global and Regional Pulse Wave Velocity Across Two MR Examinations

	σ_w (m/s)	Repeatability (m/s)
Global	0.50	1.40
Regional		
Thoracic	0.47	1.31
Mid-abdominal	0.62	1.71
Distal-abdominal	0.48	1.32

σ_w, within-subject standard deviation.

with through-plane (25) or in-plane (27) velocity encoding to quantify cross-sectional compliance and/or regional PWV. Honda et al. (22) and Resnick et al. (11) found a similar increase in compliance moving down from the thoracic to the distal-abdominal aorta in 30 (29–70 years) and 10 (44–54 years) normotensive subjects, respectively. No differences were reported by Groenink et al. (25) between regional PWVs in the thoracic and abdominal aorta of 23 normal controls aged 18–50 years, further confirming the absence of regional PWV variations in relatively young subjects.

While PWV variation along the length of the aorta has been well documented, only a few studies reported on the relationship between age and site of increased stiffening. Rogers et al. (27) found a marked interaction between age and position along the vessel, by comparing a young ($<$55 years, $n = 9$) and old ($\geq$55 years, $n = 15$) cohort of healthy volunteers. Similarly to what we have found, they showed that the thoracic aorta stiffens the most with age, followed by the mid- and distal-abdominal regions. The same conclusion was drawn by a recent MR study which compared cross-sectional compliance in the thoracic and abdominal aorta in a young (20–30 years, $n = 10$) and old (60–70 years, $n = 10$) cohort of healthy subjects (24). O'Rourke et al. found a preferential stiffening of the abdominal aorta with age, resulting in an age-related impedance matching along the length of the aorta (40). In this study, arterial stiffness was quantified in terms of the transit-time between predefined anatomical locations. However, since tortuosity of the aorta increases with age (3), quantification of arterial stiffness in terms of the transit-time only can be potentially misleading.

There is a progressive decrease in collagen and elastin content from the proximal to the distal aorta (20). Arterial elasticity is mainly determined by the balance between these two proteins, although PWV also depends on vessel wall thickness and radius, with PWV increasing with increasing wall thickness and decreasing vessel diameter. Halloran et al. (20) found that the proportion of elastin and collagen in postmortem specimens from a group of young subjects (mean age, 38 years) was similar throughout the thoracic aorta, whilst it significantly differed in the abdominal aorta. Although this finding suggested a stiffer abdominal region within this age group, we didn't observe any difference in subjects less than 40-years-old, probably due to the small sample size and the fact that the actual PWV variations are beyond the precision achievable with our measurement technique. With increasing age, degradation and fragmentation of elastin fibers occurs (41). Since the thoracic aorta is characterized by a high proportion of elastin over collagen, fracture of the elastin fibers due to fatigue induced by cyclic stresses within the aortic wall is consistent with the preferential age-related stiffening of the thoracic region found in our study. Although the structure and composition of the aortic wall play a major role in determining vascular elasticity, other factors, such as calcium deposition (42) and differential dilation of the aorta along its length (43), can influence measured indexes of aortic stiffness. As a consequence, while the presence of conflicting results in the literature is not surprising, larger cohort studies are needed to confirm our results.

Global and regional PWVs were derived from velocity data obtained using a previously reported, one-dimensional, interleaved MR pulse sequence (28). Accuracy and repeatability across two consecutive MR examinations were assessed, with the gold-standard derived from intravascular pressure measurements. Agreement between repeated MR measurements and between MR measurements and the gold-standard was good, although invasive measurements were obtained on four patients only. Bias and limits of agreement were similar to the values reported by Grotenhuis et al., who recently assessed accuracy and repeatability of CPC with through-plane velocity encoding over the arch region and the entire descending aorta (44). In the present study, however, similar values in terms of accuracy and repeatability were obtained over much shorter segments, reflecting the higher temporal and spatial resolution achieved with FVE M-mode. When testing the repeatability of our technique, the second scan was performed immediately after the first one, to minimize physiological variations. Also, after repositioning of the subject into the magnet bore, 5 to 10 minutes were allowed for the heart rate and blood pressure to settle down before the second PWV measurement was taken. The measured variation between repeated measurements was therefore probably due to slightly different prescription of the M-Mode pulse sequence on the second occasion, as every other step involved in processing of the velocity data was designed to require minimal user interaction.

The concept of spatially resolved time-velocity profiles along the vessel is of particular importance for regional PWV evaluation, when distances and transit-times are short. We have previously shown that over the entire length of the aorta FVE M-mode is more repeatable than CPC with through-plane velocity encoding (29). Similarly, Westenberg et al. recently showed that over the entire length of the aorta CPC with in-plane velocity encoding in the anterior–posterior and head-foot directions was more repeatable and accurate than CPC with through-plane velocity encoding (45). Acquisition of time-velocity profiles at multiple positions along the vessel allows visual tracking of pulse wave propagation and a more robust PWV evaluation from the slope of the line fitted to the data representing position of the foot of the wave as a function of position along the vessel.

The FVE M-mode sequence was gated to the cardiac R wave so that the obtained velocity data were effectively averaged over multiple cardiac cycles. However, since acquisition times were short, eventual misregistration artifacts due to the heart rate changing during the scan were negligible. Although the cylindrical excitation pulse used in this study was intrinsically robust to prescription errors, it can only be used within relatively straight arterial segments. While this limited our investigation to the descending region, tortuosity of the aorta in older subjects did not constitute a problem for prescription of the sequence. Another disadvantage of exciting a cylinder of magnetization centered around the vessel centerline is that the foot of the velocity waveform can be confounded by the signal arising from the static tissue surrounding the vessel. However, careful selection of the velocity sensitivity (fixed to 150 cm/s) and analysis of

the obtained velocity spectra allowed PWV measurements which were both accurate and repeatable. Ghosting artifacts due to breathing were often observed in proximity to the diaphragm. Although they did not hamper the extraction of PWV, they could have been responsible for the lower repeatability observed in the mid-abdominal region. Similarly, although eddy currents have the potential to cause systematic offsets of the velocity baseline, they are unlikely to vary quickly when moving along the aorta and therefore should have minimal effect on the determination of PWV.

CONCLUSIONS

We measured global and regional PWV in the descending aorta using FVE M-mode in a large cohort of healthy subjects. We found that the thoracic aorta stiffens the most with age, followed by the mid- and distal-abdominal regions, consistent with the theory that degradation and fragmentation of elastin fibers in the thoracic aorta cause a preferential stiffening of this region with age.

REFERENCES

1. Safar ME. Arterial stiffness: a simplified overview in vascular medicine. Adv Cardiol 2007;44:1–18.
2. McEniery CM, Yasmin, Hall IR, Qasem A, Wilkinson IB, Cockcroft JR. Normal vascular aging: differential effects on wave reflection and aortic pulse wave velocity: the Anglo-Cardiff Collaborative Trial (ACCT). J Am College Cardiol 2005;46:1753–1760.
3. Mochida M, Sakamoto H, Sawada Y, Yokoyama H, Sato M, Sato H, Oyama Y, Kurabayashi M, Tamura J, Sakamaki T. Visceral fat obesity contributes to the tortuosity of the thoracic aorta on chest radiograph in poststroke Japanese patients. Angiology 2006;57:85–91.
4. Merillon JP, Motte G, Masquet C, Azancot I, Guiomard A, Gourgon R. Relationship between physical properties of the arterial system and left ventricular performance in the course of aging and arterial hypertension. Eur Heart J 1982;3 (Suppl A):95–102.
5. Lurbe E, Torro MI, Carvajal E, Alvarez V, Redon J. Birth weight impacts on wave reflections in children and adolescents. Hypertension 2003;41(3 Part 2):646–650.
6. Tanaka H, DeSouza CA, Seals DR. Absence of age-related increase in central arterial stiffness in physically active women. Arterioscler Thromb Vasc Biol 1998;18:127–132.
7. Kingwell BA, Berry KL, Cameron JD, Jennings GL, Dart AM. Arterial compliance increases after moderate-intensity cycling. Am J Physiol 1997;273 (5 Part 2):H2186–H2191.
8. Meaney E, Samaniego V, Alva F, Valdovinos RA, Marrufo R, Vela A, Allen T, Misra A, Madsen R. Increased arterial stiffness in children with a parental history of hypertension. Pediatric Cardiol 1999;20: 203–205.
9. Benetos A, Zervoudaki A, Kearney-Schwartz A, Perret-Guillaume C, Pascal-Vigneron V, Lacolley P, Labat C, Weryha G. Effects of lean and fat mass on bone mineral density and arterial stiffness in elderly men. Osteoporos Int 2009;20:1385–1391.
10. Wiesmann F, Petersen SE, Leeson PM, Francis JM, Robson MD, Wang Q, Choudhury R, Channon KM, Neubauer S. Global impairment of brachial, carotid, and aortic vascular function in young smokers: direct quantification by high-resolution magnetic resonance imaging. J Am College Cardiol 2004;44:2056–2064.
11. Resnick LM, Militianu D, Cunnings AJ, Pipe JG, Evelhoch JL, Soulen RL. Direct magnetic resonance determination of aortic distensibility in essential hypertension: relation to age, abdominal visceral fat, and in situ intracellular free magnesium. Hypertension 1997;30(3 Part 2): 654–659.
12. Wilkinson IB, Prasad K, Hall IR, Thomas A, MacCallum H, Webb DJ, Frenneaux MP, Cockcroft JR. Increased central pulse pressure and augmentation index in subjects with hypercholesterolemia. J Am College Cardiol 2002;39:1005–1011.
13. Schram MT, Henry RM, van Dijk RA, Kostense PJ, Dekker JM, Nijpels G, Heine RJ, Bouter LM, Westerhof N, Stehouwer CD. Increased central artery stiffness in impaired glucose metabolism and type 2 diabetes: the Hoorn Study. Hypertension 2004;43:176–181.
14. Blacher J, Guerin AP, Pannier B, Marchais SJ, Safar ME, London GM. Impact of aortic stiffness on survival in end-stage renal disease. Circulation 1999;99:2434–2439.
15. Briet M, Bozec E, Laurent S, Fassot C, London GM, Jacquot C, Froissart M, Houillier P, Boutouyrie P. Arterial stiffness and enlargement in mild-to-moderate chronic kidney disease. Kidney Int 2006;69: 350–357.
16. Klocke R, Cockcroft JR, Taylor GJ, Hall IR, Blake DR. Arterial stiffness and central blood pressure, as determined by pulse wave analysis, in rheumatoid arthritis. Annals Rheumatic Dis 2003;62:414–418.
17. Booth AD, Wallace S, McEniery CM, Yasmin, Brown J, Jayne DR, Wilkinson IB. Inflammation and arterial stiffness in systemic vasculitis: a model of vascular inflammation. Arthritis Rheumatism 2004;50: 581–588.
18. Groenink M, de Roos A, Mulder BJ, Spaan JA, van der Wall EE. Changes in aortic distensibility and pulse wave velocity assessed with magnetic resonance imaging following beta-blocker therapy in the Marfan syndrome. Am J Cardiol 1998;82:203–208.
19. Laurent S, Cockcroft J, Van Bortel L, Boutouyrie P, Giannattasio C, Hayoz D, Pannier B, Vlachopoulos C, Wilkinson I, Struijker-Boudier H. Expert consensus document on arterial stiffness: methodological issues and clinical applications. Eur Heart J 2006;27:2588–2605.
20. Halloran BG, Davis VA, McManus BM, Lynch TG, Baxter BT. Localization of aortic disease is associated with intrinsic differences in aortic structure. J Surg Res 1995;59:17–22.
21. Mitchell GF, Parise H, Benjamin EJ, Larson MG, Keyes MJ, Vita JA, Vasan RS, Levy D. Changes in arterial stiffness and wave reflection with advancing age in healthy men and women: the Framingham Heart Study. Hypertension 2004;43:1239–1245.
22. Honda T, Yano K, Matsuoka H, Hamada M, Hiwada K. Evaluation of aortic distensibility in patients with essential hypertension by using cine magnetic resonance imaging. Angiology 1994;45:207–212.
23. Mohiaddin RH, Underwood SR, Bogren HG, Firmin DN, Klipstein RH, Rees RS, Longmore DB. Regional aortic compliance studied by magnetic resonance imaging: the effects of age, training, and coronary artery disease. Br Heart J 1989;62:90–96.
24. Nelson AJ, Worthley SG, Cameron JD, Willoughby SR, Piantadosi C, Carbone A, Dundon BK, Leung MC, Hope SA, Meredith IT, Worthley MI. Cardiovascular magnetic resonance-derived aortic distensibility: validation and observed regional differences in the elderly. J Hypertension 2009;27:535–542.
25. Groenink M, de Roos A, Mulder BJ, Verbeeten B, Jr, Timmermans J, Zwinderman AH, Spaan JA, van der Wall EE. Biophysical properties of the normal-sized aorta in patients with Marfan syndrome: evaluation with MR flow mapping. Radiology 2001;219:535–540.
26. Joly L, Perret-Guillaume C, Kearney-Schwartz A, Salvi P, Mandry D, Marie PY, Karcher G, Rossignol P, Zannad F, Benetos A. Pulse wave velocity assessment by external noninvasive devices and phase-contrast magnetic resonance imaging in the obese. Hypertension 2009;54:421–426.
27. Rogers WJ, Hu YL, Coast D, Vido DA, Kramer CM, Pyeritz RE, Reichek N. Age-associated changes in regional aortic pulse wave velocity. J Am College Cardiol 2001;38:1123–1129.
28. Hardy CJ, Bolster BD, Jr, McVeigh ER, Iben IE, Zerhouni EA. Pencil excitation with interleaved Fourier velocity encoding: NMR measurement of aortic distensibility. Magn Reson Med 1996;35:814–819.
29. Taviani V, Patterson AJ, Graves MJ, Hardy CJ, Worters P, Sutcliffe MP, Gillard JH. Accuracy and repeatability of Fourier velocity encoded M-mode and two-dimensional cine phase contrast for pulse wave velocity measurement in the descending aorta. J Magn Reson Imaging 2010;31:1185–1194.
30. Hardy CJ, Bottomley PA. 31P spectroscopic localization using pinwheel NMR excitation pulses. Magn Reson Med 1991;17:315–327.
31. Hardy CJ, Marinelli L, Blezek DJ, Darrow RD. MRI determination of pulse wave velocity in the carotid arteries. Proc Intl Soc Mag Reson Med 2008;16:388.
32. D'Errico J. Surface fitting using gridift. Matlab Central 2006.
33. Bland JM, Altman DG. Measurement error. BMJ 1996;313:744.
34. McDonald DA. Regional pulse-wave velocity in the arterial tree. J Appl Physiol 1968;24:73–78.
35. Guo X, Kassab GS. Variation of mechanical properties along the length of the aorta in C57bl/6 mice. Am J Physiol 2003;285:H2614–H2622.
36. Dow P, Hamilton WF. An experimental study of the velocity of the pulse wave propagated through the aorta. Am J Physiol 1939;125:60.

37. Nichols WW, McDonald DA. Wave-velocity in the proximal aorta. Med Biol Eng 1972;10:327.
38. Latham RD, Westerhof N, Sipkema P, Rubal BJ, Reuderink P, Murgo JP. Regional wave travel and reflections along the human aorta: a study with six simultaneous micromanometric pressures. Circulation 1985;72:1257–1269.
39. Ting CT, Chang MS, Wang SP, Chiang BN, Yin FC. Regional pulse wave velocities in hypertensive and normotensive humans. Cardiovasc Res 1990;24:865–872.
40. O'Rourke MF, Blazek JV, Morreels CL, Jr., Krovetz LJ. Pressure wave transmission along the human aorta. Changes with age and in arterial degenerative disease. Circ Res 1968;23:567–579.
41. Schlatmann TJ, Becker AE. Histologic changes in the normal aging aorta: implications for dissecting aortic aneurysm. Am J Cardiol 1977;39:13–20.
42. McEniery CM, McDonnell BJ, So A, Aitken S, Bolton CE, Munnery M, Hickson SS, Yasmin, Maki-Petaja KM, Cockcroft JR, Dixon AK, Wilkinson IB. Aortic calcification is associated with aortic stiffness and isolated systolic hypertension in healthy individuals. Hypertension 2009;53:524–531.
43. Virmani R, Avolio AP, Mergner WJ, Robinowitz M, Herderick EE, Cornhill JF, Guo SY, Liu TH, Ou DY, O'Rourke M. Effect of aging on aortic morphology in populations with high and low prevalence of hypertension and atherosclerosis. Comparison between occidental and Chinese communities. Am J Pathol 1991;139:1119–1129.
44. Grotenhuis HB, Westenberg JJ, Steendijk P, van der Geest RJ, Ottenkamp J, Bax JJ, Jukema JW, de Roos A. Validation and reproducibility of aortic pulse wave velocity as assessed with velocity-encoded MRI. J Magn Reson Imaging 2009;30:521–526.
45. Westenberg JJ, Hendriksen D, Steendijk P, van der Geest RJ, Grotenhuis HB, Groenink M, Jukema JW, De Roos A, Reiber JH. Improved aortic pulse wave velocity assessment with in plane velocity-encoded MRI: validation and reproducibility. Proc Intl Soc Mag Reson Med 2009;17:3851.